

Active processes make mixed lipid membranes either flat or crumpled

Tirthankar Banerjee^{1,*} and Abhik Basu^{1,2,†}

¹*Condensed Matter Physics Division, Saha Institute of Nuclear Physics, Calcutta 700064, India*

²*Max-Planck Institut für Physik Komplexer Systeme,
Nöthnitzer Str. 38, Dresden, D-01187 Germany*

(Dated: July 3, 2021)

Whether live cell membranes show miscibility phase transitions (MPTs), and if so, how they fluctuate near the transitions remain outstanding unresolved issues in physics and biology alike. Motivated by these questions we construct a generic hydrodynamic theory for lipid membranes that are active, due for instance, to the molecular motors in the surrounding cytoskeleton, or active protein components in the membrane itself. We use this to uncover a direct correspondence between membrane fluctuations and MPTs. Several testable predictions are made: (i) generic *active stiffening* with orientational long range order (flat membrane) or *softening* with crumpling of the membrane, controlled by the *active tension* and (ii) for mixed lipid membranes, capturing the nature of putative MPTs by measuring the membrane conformation fluctuations. Possibilities of both first and second order MPTs in mixed active membranes are argued for. Near second order MPTs, active stiffening (softening) manifests as a *super-stiff (super-soft) membrane*. Our predictions are testable in a variety of *in-vitro* systems, e.g., live cytoskeletal extracts deposited on liposomes and lipid membranes containing active proteins embedded in a passive fluid.

I. INTRODUCTION

Cell membranes are generally made of several lipids and have complex structures [1]. The dynamics of cell membranes are affected by biological active (nonequilibrium) processes (e.g., nonequilibrium fluctuations of cell cytoskeletons [2] and active proteins in the lipid membrane [3]); see also Ref. [4]. Miscibility phase transitions (MPTs) in equilibrium heterogeneous or mixed model lipid bilayers and giant plasma membrane vesicles (GPMVs) are well studied [5, 6]. In contrast, occurrence of MPTs in eukaryotic cell membranes, remains controversial till date [7]. Whether cellular active processes can control membrane fluctuations and associated MPTs in mixed membranes and if so, how, form general motivations for the present study.

Structural and dynamical complexities of cell membranes preclude simple physical understanding of MPTs in cell biological context. This calls for studying this question within a simpler nonequilibrium model appropriate for an in-vitro setting, where this issue may be addressed systematically and possibly verified in suitably designed *in-vitro* experiments. To this end, in this article we construct a hydrodynamic theory for planar active mixed lipid (fluid) membranes [1]. Hydrodynamic approaches have a long history of applications in both equilibrium [8, 9] and nonequilibrium [10, 11] systems and are successful in predicting general physical properties at large scales independent of the microscopic (molecular) details of the systems. In particular, our theory is applicable to a variety of systems, e.g., a lipid bilayer in an orientable active fluid [10] in its isotropic phase [12] or a lipid bilayer with an active component, e.g., active proteins, immersed in a passive fluid [3]. We use it to study the membrane conformation fluctuations and the associated active or nonequilibrium MPTs. Both second order MPT (through critical and tricritical points), and first order MPT are considered. We uncover a *direct correspondence* between membrane fluctuations and the nature of the MPTs, potentially opening up a new experimental route to study the MPTs. Our predictions are quite general; we expect that our characterisations of the membrane fluctuations and MPTs should serve as references for experimental observations on MPTs in mixed model lipid bilayers and GPMVs in isotropic actomyosin extracts with adenosine triphosphate (ATP) molecules or solutions of live orientable bacteria [13], and lipid membranes with active protein inclusions embedded in passive fluids. From perspectives of nonequilibrium physics, our model provides an intriguing example where the same underlying microscopic active processes control two distinct phenomena, *viz.* MPTs of the membrane composition and the nature of fluctuations of the membrane conformation, ultimately linking the two in a definitive way.

In order to focus on the essential physics of the problem, we consider a planar, tensionless, two-component, inversion-symmetric [14], single-layered lipid membrane [15] of linear size L . In stark contrast to equilibrium lipid membranes [16,

*Electronic address: tirthankar.banerjee@saha.ac.in

†Electronic address: abhik.basu@saha.ac.in, abhik.123@gmail.com

17], our model membrane displays generic stiffening and statistical flatness for positive active tensions σ_a , but softening and crumpling for $\sigma_a < 0$ at any temperature T . We describe the planar membrane conformations by a single-valued height field $h(\mathbf{x}, t)$ in the Monge gauge [9, 18], in two dimensions ($2d$) with the local normal $\mathbf{n} = (-\nabla h, 1) = (\delta\mathbf{n}, 1)$ [9, 18]. Then, for positive σ_a , away from the critical point for second order MPT and across first order MPT we find variances

$$\Delta_n = \langle (\delta\mathbf{n}(\mathbf{x}, t))^2 \rangle \sim \text{const.}, \quad (1)$$

$$\Delta_h = \langle h(\mathbf{x}, t)^2 \rangle \sim \ln L, \quad (2)$$

in the thermodynamic limit (TL). These imply orientational long range order (LRO), hence statistical flatness and positional quasi long range order (QLRO); here $\langle \dots \rangle$ implies averaging over noises; see dynamical equations (8) and (9), respectively, below. Near the critical point, the membrane becomes *super stiff*: in a mean-field like treatment, we show

$$\Delta_h \sim \ln \ln L, \quad (3)$$

in TL, an L -dependence weaker than in QLRO, which we call positional *nearly long range order* (NLO). Moreover, Δ_n is further suppressed near the critical point. In contrast, for $\sigma_a < 0$, Δ_n and Δ_h diverge for membranes larger than a *persistence length*, i.e., $L > \zeta$ [17], indicating orientational and positional short range orders (SRO). The rest of this article is organised as follows. In Sec. II, we set up our coarse-grained equations of motion. Then in Sec. III we discuss our results on the membrane conformation fluctuations at or across various MPTs. Section IV discusses the various MPTs possible within our model. Finally, in Sec. V we summarise our results. A glossary of our results has been added in Sec. VI for the convenience of the readers. Some technical aspects of the calculations involved and a few additional discussions related to the main results of this work are made available in Appendices A to G for interested readers.

II. CONSTRUCTION OF THE MODEL

We consider an incompressible mixed permeable membrane composed of two lipids A and B of equal amount with local concentrations $n_A(\mathbf{x}, t)$ and $n_B(\mathbf{x}, t)$, respectively [17], $n_A + n_B = 1$. The local inhomogeneity $\phi (= n_A - n_B)$ is the order parameter for the MPT. Since the active processes may in general interact differently with A and B, we relax the usual inversion symmetry of ϕ for a binary mixture [19] when coupled to local mean curvatures in the present model (see Refs. [17, 20, 21] in this context).

Now, consider a nearly flat permeable membrane spread parallel to the xy -plane, i.e., with local normals parallel to the z -axis on average; see Fig. 1 for a schematic diagram. While the height field h is a nonconserved broken

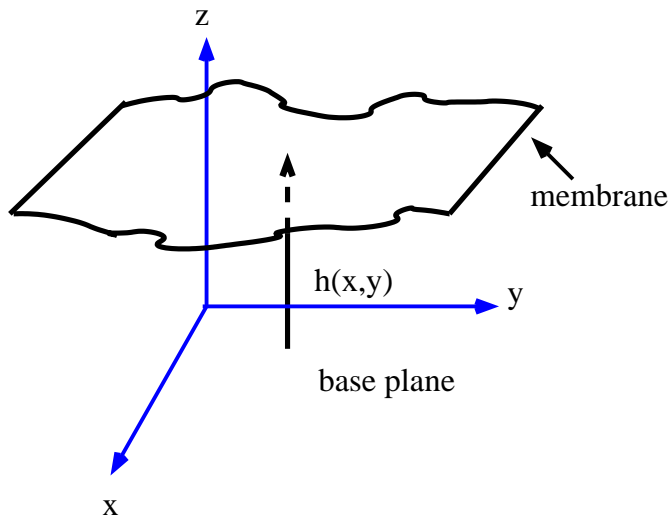


FIG. 1: Schematic configuration of the nearly flat model membrane in the Monge gauge. The membrane is surrounded by bulk fluid above and below.

symmetry variable, the order parameter field ϕ is a conserved density, since n_A and n_B are conserved. The relevant

equations of motion for h and ϕ may be derived as follows. The membrane, treated as a permeable fluid film [22], has a local velocity in the normal direction (along z direction in this case) v_{mz} given by

$$v_{mz} = v_{hydro_z} + v_{perm}. \quad (4)$$

Here, v_{hydro_z} is the z -component of the local three-dimensional (3d) hydrodynamic velocity \mathbf{v}_{hydro} [12], and v_{perm} represents the local permeative flows [12]. In general, both v_{perm} and \mathbf{v}_{hydro_z} may contain equilibrium (controlled by a free energy \mathcal{F} ; see below) and active parts. The latter contributions cannot be obtained from \mathcal{F} . Instead, symmetry considerations (e.g., translation, in-plane rotation, inversion symmetry of h and invariance under tilt for the membrane) may be used to enforce the general forms of the active contribution to v_{perm} . We write

$$v_{perm} = \Gamma_h(\lambda\phi^2 + \tilde{\lambda}\phi)\nabla^2 h - \mu_p \frac{\delta\mathcal{F}}{\delta h} \quad (5)$$

to the lowest order in nonlinearities and gradients satisfying the relevant invariances. The first term on the rhs of (5) with coefficients λ and $\tilde{\lambda}$ is the active contribution to v_{perm} ; μ_p is a (constant) kinetic coefficient for the equilibrium contribution to the permeative flows. The active terms with coefficients λ and $\tilde{\lambda}$ are forbidden in equilibrium due to the tilt invariance of the associated free energy \mathcal{F} (see below) [17]. They are, however, permitted here as the tilt invariance in the present problem must hold at the level of the equations of motion [11]. All of $\lambda, \tilde{\lambda}, \mu_p$ vanish for impermeable membranes. Furthermore, λ and $\tilde{\lambda}$ control the strength of σ_a , the active tension (see below); a non-zero $\tilde{\lambda}$ models the asymmetric dependence of the active processes on lipids A and B. Symmetry arguments cannot determine the signs of $\lambda, \tilde{\lambda}$. In this work, we examine the consequences of both positive and negative λ ; the sign of $\tilde{\lambda}$ can be absorbed within the definition of ϕ . Further, for a membrane with a fixed background there are no active contributions to v_{hydro_z} that are more relevant than the $\lambda, \tilde{\lambda}$ -terms above [23]; $v_{hydro_z} = -\Gamma_0\delta\mathcal{F}/\delta h$ with kinetic coefficient Γ_0 being a constant. The dynamics of ϕ should generally follow a conservation law form advection-diffusion equation [8]. To proceed further, we assume \mathcal{F} for a tensionless, mixed lipid membrane to have the simple generic form

$$\begin{aligned} \mathcal{F} = & \int d^d x \left[\frac{\kappa}{2}(\nabla^2 h)^2 + \lambda_1\phi^2(\nabla^2 h)^2 + \lambda_2\phi(\nabla^2 h)^2 \right. \\ & \left. + \frac{r}{2}\phi^2 + \frac{1}{2}(\nabla\phi)^2 + \frac{g}{3}\phi^3 + \frac{u}{4!}\phi^4 + \frac{v}{6}\phi^6 - \tilde{h}\phi \right]. \end{aligned} \quad (6)$$

Here $r = T - T_c$, $u, v > 0$. Couplings g and \tilde{h} can be of either sign; for a symmetric binary mixture $g = 0 = \tilde{h}$. Coupling v has been added for reasons of thermodynamic stability (see below) and is irrelevant in equilibrium with $u > 0$. Free energy (6) without membrane fluctuations ($h = \text{const.}$) describes MPTs identical to the standard liquid-gas phase transition that is generally first order in nature, and admits a second order MPT at a critical point that can be accessed only by setting $T = T_c$ and also tuning h to a critical value (equivalently setting pressure $p = p_c$, the critical pressure), in analogy with magnetic systems [9]. This analogy can be made more precise by expanding \mathcal{F} about $\phi = \phi_0$, with ϕ_0 is chosen such that the $g\phi^3$ -term in \mathcal{F} above vanishes. The resulting transformed free energy has the form same as that of the Ising model at a finite external magnetic field \tilde{h}_0 (related to \tilde{h} and depends upon the chemical potential and temperature) that has generic first order MPTs (or may show no transitions) if \tilde{h}_0 is tuned at any general T ; furthermore, second order MPT belonging to the $2d$ Ising universality class is found if *both* T and \tilde{h}_0 are tuned; the corresponding critical point is located in a $T - \tilde{h}_0$ -plane at $r = 0$ or $T = T_c$ (in a mean-field description) and $\tilde{h}_0 = 0$ [9]. In fact, the path in the temperature - pressure plane of a binary mixture that directly resembles the zero magnetic field path in a magnet (which shows a second order transition) is the one with the density fixed at the critical density, i.e., the critical isochore. Notice that the coexistence curve for \mathcal{F} above is similar to that for the Ising model, except now being asymmetric with respect to the order parameter $\langle\phi\rangle = m$ due to the lack of any symmetry of \mathcal{F} under inversion of ϕ [9]. The inclusion of h -fluctuations in (6) via the couplings λ_1, λ_2 does not alter this picture [6, 17]. This may be easily seen from the form of \mathcal{F} : the λ_1 and λ_2 terms effectively only induce fluctuation-corrections to r and \tilde{h} , respectively. To what degree this equilibrium physical picture is affected by the activity remains to be seen (see below).

Notice that \mathcal{F} implies an effective composition-dependent bending modulus $\tilde{\kappa}(\phi)$ of the form [17]

$$\tilde{\kappa}(\phi) = \kappa + 2\lambda_1\phi^2 + 2\lambda_2\phi. \quad (7)$$

Parameters λ_1, λ_2 should be chosen to ensure $\tilde{\kappa}(\phi) > 0$ for all ϕ , that guarantees a thermodynamically stable flat phase, given by the minimum of \mathcal{F} , in equilibrium. We choose $\lambda_1 > 0$ [17]. The sign of λ_2 is arbitrary and can be absorbed within the definition of ϕ ; for concreteness we choose $\lambda_2 > 0$. While the individual signs of $\tilde{\lambda}$ and λ_2 are

arbitrary, the sign of the product $\lambda_p \equiv \tilde{\lambda}\lambda_2$ is crucial to what follows below and controls the ensuing macroscopic behaviour.

Putting together everything, the dynamical equations for h (with $\partial_t h = v_{mz}$) and ϕ to the lowest order in spatial gradient expansions, in the long wavelength limit take the forms (for a fixed background medium)

$$\frac{\partial h}{\partial t} = \Gamma_h[-\kappa\nabla^4 h + (\lambda\phi^2 + \tilde{\lambda}\phi)\nabla^2 h] + f_h, \quad (8)$$

$$\begin{aligned} \frac{\partial \phi}{\partial t} = & \Gamma_\phi \nabla^2 [r\phi - \nabla^2 \phi + \frac{u}{3!}\phi^3 + 2\lambda_1\phi(\nabla^2 h)^2 \\ & + \lambda_2(\nabla^2 h)^2 + v\phi^5] + \nabla \cdot \mathbf{f}_\phi. \end{aligned} \quad (9)$$

Notice that the terms with coefficients λ_1, λ_2 in (6) generate additional equilibrium terms in (8); these are however subleading in the hydrodynamic limit (in a scaling sense) to the active $\lambda, \tilde{\lambda}$ -terms, respectively, and are hence omitted from (8) [25]. Kinetic coefficient $\Gamma_h = \mu_p + \Gamma_0$ is a constant for a membrane with a fixed background; Γ_ϕ is also a constant. Notice that separately Eq. (9) may be wholly obtained from \mathcal{F} and is just of the “model B” conservation law form (in the nomenclature of Ref. [8]); this is because there are no active terms which are more relevant (in a scaling sense) than those already included in (9). In fact, the λ_1 - and λ_2 - nonlinear terms in (9) originate from the composition-dependent bending modulus $\kappa(\phi)$ in (7) in the free energy (6). This does not, however, in general imply that ϕ follows an equilibrium dynamics; its coupling with h ensures that the resulting effective dynamics for ϕ is detailed balance breaking. Further, we have ignored any in-plane advection of ϕ for simplicity [26]. Noises f_h and \mathbf{f}_ϕ are zero-mean, Gaussian distributed with variances given by

$$\langle f_h(\mathbf{q}, \omega) f_h(\mathbf{q}', \omega') \rangle = 2D_h \Gamma_h \delta(\mathbf{q} + \mathbf{q}') \delta(\omega + \omega'), \quad (10)$$

$$\langle f_{\phi i}(\mathbf{q}, \omega) f_{\phi j}(\mathbf{q}', \omega') \rangle = 2D_\phi \Gamma_\phi \delta_{ij} \delta(\mathbf{q} + \mathbf{q}') \delta(\omega + \omega'). \quad (11)$$

Here, $D_h \neq D_\phi$ in general; \mathbf{q}, \mathbf{q}' are wavevectors and ω, ω' are frequencies, $q = |\mathbf{q}|$. Noises f_h and $f_{\phi i}$ should contain both thermal as well as active contributions.

A. Active terms

The dynamical equations (8) and (9) are constructed using symmetry arguments. As a result, these serve as good hydrodynamic representations for a variety of systems that conform to the same symmetries as Eqs. (8) and (9). Equivalently, the active terms in (8) can be motivated in various physical contexts. For instance, consider an inversion-symmetric, mixed, planar fluid membrane placed in an isotropic, active suspension of actin filaments [10], grafted normally to it. This is imposed by the condition $\mathbf{p} \cdot \mathbf{n} = 1$, where \mathbf{p} is the local orientation or director fields [27] which describe the local orientation of the actin filaments. This yields $p_j = \partial_j h$ ($j = x, y$) to the linear order in height fluctuations [28] at the location of the membrane ($z = h$). In the embedding bulk isotropic active medium, there is no net orientational order and hence the fluctuations of \mathbf{p} relax *fast* [12, 29]. Thus, \mathbf{p} in the bulk are not hydrodynamic variables and can be ignored in the long time limit as far as the bulk embedding fluid is concerned. At $z = h$, the location of the membrane, however, \mathbf{p} is nonzero and is slaved to the membrane fluctuations, as above. The general form of the z -component of the local membrane velocity, taking into account the permeative flow, is

$$\begin{aligned} \frac{\partial h}{\partial t} = & v_z(z = h) = -\mu_p \delta \mathcal{F} / \delta h + X(\phi) \partial_j (p_z p_j) + v_{hydroz} \\ = & -\Gamma_h \delta \mathcal{F} / \delta h + X \nabla^2 h \end{aligned} \quad (12)$$

at the lowest order in fluctuations (see Ref. [12] for a similar active contribution), consistent with the inversion-symmetry. Now, with $X(\phi) = \Gamma_h(\lambda\phi^2 + \tilde{\lambda}\phi)$ [30] and $p_z = 1$ to the leading order in smallness, we recover (8). That this local orientation fluctuation gives rise to active permeation flows is not surprising: the polymerisation/depolymerisation and treadmilling of the actin filaments, which are active processes [1, 12, 31], pull or push the membrane. This contributes to the permeation flow and can either reinforce or oppose the corresponding equilibrium contribution. Yet another system that may be described by (8) and (9) is the hydrodynamics of permeable lipid membranes with active protein inclusions [3, 32] that are either embedded in the bilayer or adsorbed to it (e.g., cytoskeleton proteins) and can phase separate, immersed in a passive fluid. These active proteins convert chemical energy of the ATP molecules or of the light shone [33] on the membrane into mechanical motion of the membrane. Local order parameter ϕ in such systems should describe the mole fraction of the active components. The main physical features of these active proteins are that they force the membrane locally and independently of each other,

generating a local normal motion of the membrane that should evidently depend upon ϕ [32]. The active terms in (8) then simply model the ϕ -dependence of the local normal velocity of the membrane. This ϕ -dependence leads to the active tension σ_a ; see below.

Now imagine regions of nonzero mean curvature with excess lipid of one kind so that ϕ picks up a non-zero value with a specific sign. Such a region then either pulls up the curved region further (instability) or tries to flatten the curvature (stable membrane) due to the active processes; see Fig. 2 for a schematic picture. For an active fluid with

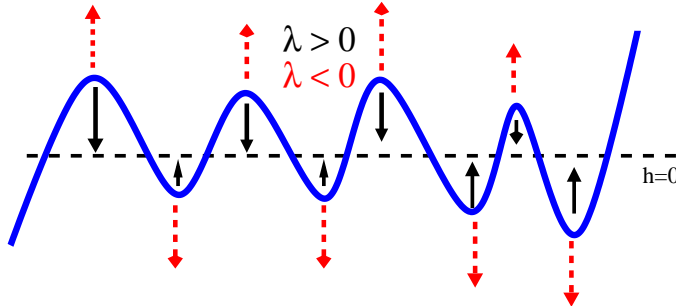


FIG. 2: (Color online) Schematic representations of the active velocity ($\tilde{\lambda} = 0$) of the membrane (blue curved line) for $\lambda > 0$ (stabilising, solid black arrows) and $\lambda < 0$ (destabilising, broken red arrows). A non-zero $\tilde{\lambda}$ leads to further ϕ -dependent modification of the active velocity (not shown).

actin filaments, $\lambda, \tilde{\lambda}$ should scale with the concentration C_0 of the ATP molecules and the free energy released in hydrolysis of ATP, $\Delta\mu \sim 0.8 \times 10^{-18} kJ$ [34]. In the example of a live cytoskeletal extract, active contributions to v_{perm} should depend on the treadmilling speed of the actin filaments $\sim O(1 \mu m/h)$ [35]; this may be used to make an estimate on $\lambda, \tilde{\lambda}$. For a membrane with an active component, $\lambda, \tilde{\lambda}$ should scale with the mean concentration of the active species in the membrane.

It is now instructive to compare and contrast with the generic leading order active terms present for a pure tensionless membrane ($\phi = 0$). For a pure membrane, the leading order active propulsion velocity is just a constant: $X(\phi = 0) = \Gamma_h \alpha$ to the leading order. Thus, for such a pure membrane with a vanishing tension in an active medium, the dynamical equation for h can be obtained from an effective free energy that now includes an *effective surface tension* $\sigma' = \alpha$ in the free energy. We can write

$$\frac{\partial h}{\partial t} = -\Gamma_h \frac{\delta F_h}{\delta h} + v_{hydroz} + f_h, \quad (13)$$

where $F_h = \int d^2x [\sigma'(\nabla h)^2/2 + \kappa(\nabla^2 h)^2/2]$. Thus, for a symmetric pure membrane, the active effects may be wholly described by a modified equilibrium free energy F_h to the leading order, or, equivalently, the role of active effects here is to just to introduce an effective surface tension. For a mixed membrane, there is no such general equivalence with a simply modified equilibrium model.

III. RESULTS

In this Sec. we first derive our results on membrane fluctuations without any (equilibrium) surface tension by using the model equation (8). We analyse Eq. (8) in a mean field-like spirit and compare its properties with an isolated tensionless fluid membrane at thermal equilibrium. We then establish their correspondence with the order of MPTs, the principal prediction of this work. Next, we briefly touch upon how a finite surface tension may affect our results. We now proceed to discuss these in details below.

A. Properties of membrane fluctuations

The lack of knowledge about the order of MPTs in a symmetric mixed membrane embedded in an active fluid, demands that we must allow for the possibility of both first order MPT and second order MPT, and study their connections with the membrane fluctuations separately; see Ref. [36] for a recent study of first order MPT in a lipid bilayer in presence of transmembrane proteins. In particular, this opens the intriguing possibility of activity-induced first order MPT in a mixed lipid bilayer that admits only second order MPT in the equilibrium limit. We present

theoretical arguments in favour of both first order MPTs and second order MPTs later in the text. From (8), we extract an *active tension* σ_a . We write in the Fourier space

$$\frac{\partial h}{\partial t} = \Gamma_h [-\kappa q^4 h - X(\phi) q^2 h] + f_h, \quad (14)$$

where $X(\phi) = \lambda \phi^2 + \tilde{\lambda} \phi$; \mathbf{q} is a Fourier wavevector. Now write $X(\phi) = \langle X(\phi) \rangle + \delta X(\phi)$; $\delta X(\phi)$ is the fluctuation of $X(\phi)$ about its mean $\langle X(\phi) \rangle$. Then, neglecting $\delta X(\phi)$ in comparison with $\langle X(\phi) \rangle$ for (assumed) small fluctuations (in mean-field like treatment) and for any $\lambda \neq 0$, we can extract an *active tension* σ_a as follows:

$$\sigma_a = \lambda \langle \phi^2 \rangle, \quad (15)$$

with $\langle \phi \rangle = 0$ for the whole system with equal A and B at all T ; clearly σ_a is positive (negative) for $\lambda > (<) 0$. Consider $\lambda > 0$ first. Equations (14) and (15) imply for the membrane height fluctuations

$$C_h(q) = \langle |h(\mathbf{q})|^2 \rangle = \frac{D_h}{\sigma_a q^2 + \kappa q^4}. \quad (16)$$

Thus $C_h(q)$ is dominated by the active tension $\sigma_a q^2 > 0$ in the long wavelength limit, since κq^4 is subleading to it (in a scaling sense). At this stage it is formally instructive to compare $C_h(q)$ as given in (16) with that of a tensionless fluid membrane (since our model membrane has zero surface tension in equilibrium) with an *effective bending modulus* κ_e in equilibrium at temperature $D_h/(\Gamma_h K_B)$. This yields

$$\kappa_e(q) = \kappa + \frac{\sigma_a}{q^2} = \kappa + \frac{\lambda}{q^2} \langle \phi^2 \rangle. \quad (17)$$

Unsurprisingly, $\kappa_e(q)$ has a part that diverges as $1/q^2$, a reflection of the active tension $\sigma_a(q)$, that is dimensionally identical to the usual surface tension. Equivalently, to the leading order our tensionless model active membrane behaves like an equilibrium membrane under tension. This suggests generic stiffening (softening) of the model membrane for $\lambda > (<) 0$ at *any* T , in contrast to an isolated fluid membrane in equilibrium [17]. Positive and negative λ , respectively, physically imply that creation of nonuniform regions with specific signs of ϕ (i.e., A- or B-rich domains) should make the membrane either try to flatten out ($\sigma_a > 0$), or curve more ($\sigma_a < 0$); see also Refs. [4, 12] for active tension in different models for active membranes. Now assume $\lambda > 0$. In the ordered phase, $\langle \phi^2 \rangle = m^2$ (neglecting fluctuations) is larger than its value in the disordered phase; hence $\kappa_e(q) > \kappa$ in the ordered phase, where m is the average of ϕ in an A- or B-rich domain in the ordered phase.

For a putative first order MPT at $T = T^*$, we write

$$\begin{aligned} \sigma_a(q) = \lambda \langle \phi^2 \rangle &\implies \kappa_e(q) = \kappa + \lambda \langle \phi^2 \rangle / q^2 \quad (T > T^*), \\ \sigma_a(q) = \lambda m^2 &\implies \kappa_e(q) = \kappa + \lambda m^2 / q^2 \quad (T < T^*), \end{aligned} \quad (18)$$

ignoring ϕ -fluctuations in comparison with m^2 for $T < T^*$. Thus there is a *jump* in κ_e , that is large for small q , as T crosses T^* . Now,

$$\Delta_h = D_h \int_{2\pi/L}^{\Lambda} \frac{d^2 q_1}{\kappa_e q_1^4} \approx \tilde{A} \ln L \quad (19)$$

in TL, implying positional QLRO, where, \tilde{A} is a nonuniversal constant with a value dependent upon ordered and disordered phases; $\tilde{A} = \frac{D_h}{2\pi\lambda m^2}$ (for $T < T^*$); see Eq. (2). Here, \mathbf{q}_1 is a wavevector; $|\mathbf{q}_1| = q_1$; Λ is an upper wavevector cut-off. With Eq. (15),

$$\Delta_n = D_h \int_{2\pi/L}^{\Lambda} \frac{q_1^2 d^2 q_1}{(2\pi)^2 \kappa_e q_1^4} \quad (20)$$

is finite in TL (i.e., orientational LRO), independent of the nature of MPTs. Note that both Δ_n , Δ_h are *discontinuous* across T^* , due to the discontinuity in $\kappa_e(q)$ across first order MPT.

In contrast, for second order MPT $\langle \phi^2 \rangle$ changes continuously on both sides of $T = T_c$ and rises as $|r(T)|$ becomes smaller. Thus $\kappa_e(q)$, as given by (15), rises smoothly as T_c is approached from either side; see Fig. III A.

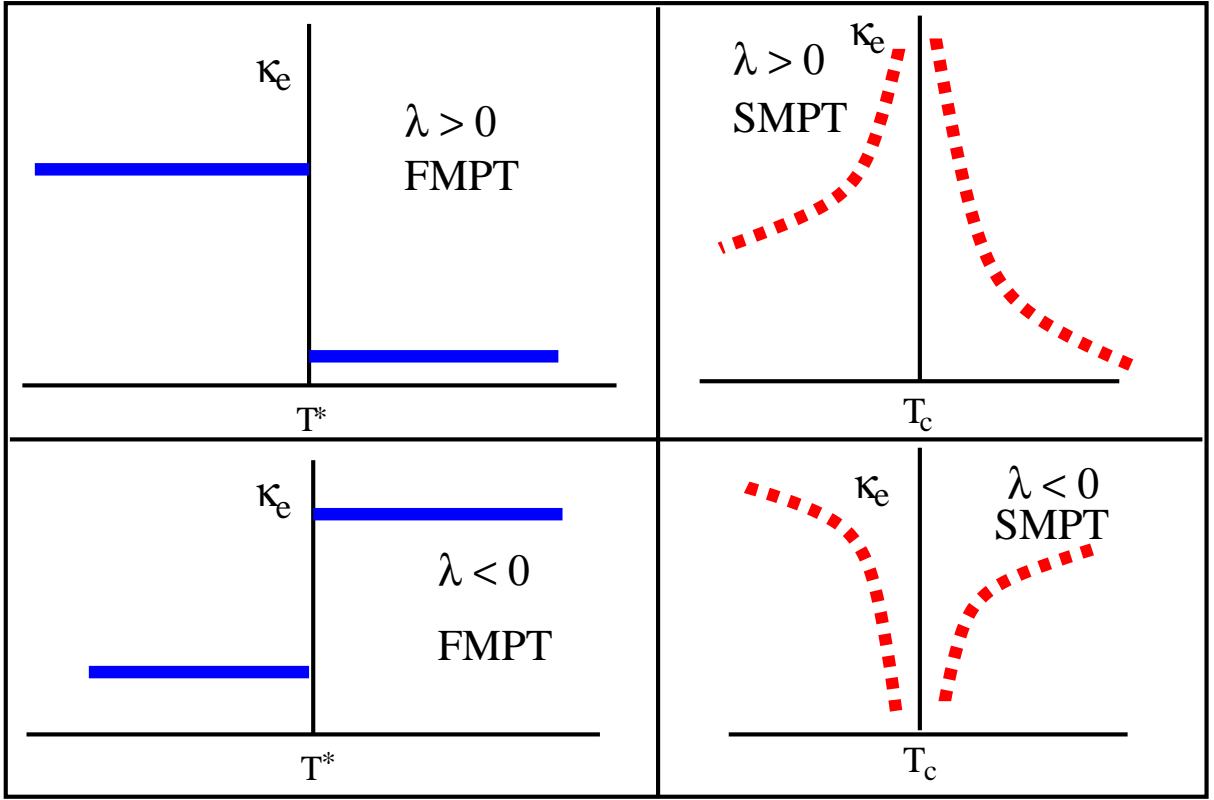


FIG. 3: (Color online) Schematic variation of $\kappa_e(q = q_0)$ across first order MPT (left) and second order MPT (right) for both $\lambda > 0$ ($\sigma_a > 0$) (top) and $\lambda < 0$ ($\sigma_a < 0$) (bottom) with $q_0 = 2\pi/L$; membrane size L is chosen such that $\kappa_e(q_0) > 0$ with $\lambda < 0$, or $L < \zeta$, the persistence length. Smooth (discontinuous) variations of κ_e across T_c (T^*) are shown (see text).

For $T > T_c$,

$$\kappa_e(q) \approx \frac{\lambda D_\phi}{4\pi^2 q^2} \int_{2\pi/L}^{\Lambda} \frac{d^2 q_1}{r + q_1^2} = \frac{\lambda D_\phi}{4\pi q^2} \ln \left| \frac{r + \Lambda^2}{r} \right|. \quad (21)$$

This yields

$$\Delta_h = \tilde{G} \ln L \quad (22)$$

in TL, implying positional QLRO for $T > T_c$; giving Eq. (2) above; $\tilde{G} = \frac{2D_h}{\lambda D_\phi \ln | \frac{r + \Lambda^2}{r} |}$, a nonuniversal constant, different from \tilde{A} . For $T < T_c$ as well, positional QLRO holds, however, with a different nonuniversal value for \tilde{G} . For both $T > T_c$ and $T < T_c$,

$$\Delta_n = \int_{2\pi/L}^{\Lambda} \frac{d^2 q}{(2\pi)^2} \frac{D_h}{\kappa_e q^2} \quad (23)$$

remains finite in TL. However, unlike for first order MPT, both Δ_n and Δ_h are continuous across T_c for second order MPT. Variations of $\kappa_e(q)$ around first order MPT and second order MPT for a given q are shown schematically in Fig. III A; also see Glossary at the end summarising our results on $\kappa_e(q)$, Δ_n , Δ_h across MPTs.

Care must be taken while analysing the membrane fluctuations close to the critical point: large ϕ -fluctuations very close to the critical point should qualitatively change $\sigma_a(q)$ and hence $\kappa_e(q)$. For simplicity, set $\lambda = 0 = \lambda_2$, such that the Ising symmetry for ϕ is restored. This suffices for our purposes here, since we are interested in second order MPT only. From (15) with $\lambda > 0$ and within a linearised approximation to Eq. (9), we find near the critical point ($r \approx 0$)

$$\begin{aligned} \sigma_a(q) &= -\frac{\lambda D_\phi}{2\pi} \ln q \\ \Rightarrow \kappa_e(q) &= \kappa - \frac{\lambda D_\phi}{2\pi q^2} \ln q \approx -\frac{\lambda D_\phi}{2\pi q^2} \ln q, \end{aligned} \quad (24)$$

for small q ; see Appendix for a renormalised version of Eq. (24). Then,

$$\Delta_n = -\frac{D_h}{\lambda D_\phi} \int_{2\pi/L}^\Lambda \frac{q dq}{\ln q} \sim \text{finite} \quad (25)$$

and

$$\Delta_h = (D_h/\lambda D_\phi) \ln \ln L \quad (26)$$

in TL. This establishes orientational LRO and positional NLO, respectively, with $D_h/(\lambda D_\phi)$ as the nonuniversal amplitude; see Eq. (3). Thus at T_c , Δ_n is further suppressed from its value at $T \neq T_c$, yielding a *super-stiff* membrane at the critical point. This result holds with or without the ambient fluid hydrodynamics. A schematic phase diagram in the $\lambda - T$ plane is shown in Fig. 5. These are in stark contrast with their equilibrium results. In equilibrium Δ_n scales as $\ln \ln L$ at $T = T_c$ [17], displaying orientational NLO; at all other T , a pure membrane in equilibrium does not remain flat at large scales [17].

For $\lambda < 0$, we have $\sigma_a < 0$. Hence $\kappa_e(q) < 0$ for sufficiently low q , implying long wavelength instability for planar membranes or occurrence of *membrane crumpling*. In general, larger $\langle \phi^2 \rangle$ in the ordered phase leads to a smaller $\kappa_e(q)$. We define a persistence length ζ , such that for $q = 2\pi/\zeta$, $\kappa_e(\zeta) = 0$ [17, 37]. This clearly indicates instability of flat membranes, and as argued in Ref. [16], the membrane gets crumpled. Physically, for length scales $L < \zeta$ the membrane appears flat on average, where as for $L > \zeta$, it is crumpled. The strong dependence of κ_e on the nature of the transition (first order MPT or second order MPT) is also reflected in ζ . In particular, across an first order MPT at T^* ,

$$\begin{aligned} \zeta &= 2\pi \sqrt{\frac{\kappa}{|\lambda| \langle \phi^2 \rangle}}, \text{ for } T > T^* \text{ and} \\ \zeta &= 2\pi \sqrt{\frac{\kappa}{|\lambda| m^2}} \text{ for } T < T^*, \end{aligned} \quad (27)$$

thus showing a jump in ζ ; in general $\zeta(T > T^*) > \zeta(T < T^*)$. In contrast, there is no discontinuity in ζ for second order MPT at $T = T_c$: ζ satisfies

$$\zeta^2 \ln[\zeta/(2\pi)] = \frac{8\pi^3 \kappa}{D_\phi |\lambda|} \quad (28)$$

at T_c . Away from $T = T_c$, $\zeta(T > T_c) > \zeta(T < T_c)$, similar to the behaviour of ζ across $T = T^*$ in first order MPT. Both Δ_n and Δ_h diverge at finite $L \sim \zeta$, implying orientational and positional SRO. Due to the large fluctuations of ϕ at the critical point, $\zeta(T_c) \ll \zeta(T \neq T_c)$, giving *super-crumpling* of the membrane, in contrast to super stiffness for $\lambda > 0$ at the critical point; see Appendix for more details.

B. Correspondence between membrane fluctuations and order of MPTs - experimental implications

Consider now the implications of the above results on the measurements of membrane conformation fluctuations. These may be measured by standard spectroscopic methods, see, e.g., Ref. [38]. Notice that the knowledge of the behaviour of $\sigma_a = \lambda \langle \phi^2 \rangle$, or $\kappa_e(q) \equiv \kappa + \lambda \langle \phi^2 \rangle / q^2$ immediately enables us to find the scaling of $C_h(q) = D_h/(\sigma_a q^2 + \kappa q^4)$ across second order MPT or first order MPT, that can be measured in experiments. We make the following general conclusions:

(i) With second order MPT at both $T > T_c$ or $T < T_c$, $C_h(q) \sim 1/q^4$ for large q , where as $C_h(q) \sim 1/q^2$ for small q and $\lambda > 0$; $C_h(q)$ diverges for $q \rightarrow 0$ only with no finite wavevector singularities. Further, since $\sigma_a(T < T_c) > \sigma_a(T > T_c)$, $C_h(q)(T < T_c) < C_h(q)(T > T_c)$ for sufficiently small q , when $\sigma_a q^2$ dominates over κq^4 . Furthermore, the difference $C_h(q)(T > T_c) - C_h(q)(T < T_c)$ vanishes as $T \rightarrow T_c$, i.e., $C_h(q)$ has no discontinuity as a function of T , in agreement with the continuity of σ_a or κ_e across T_c .

(ii) In contrast, for $\lambda < 0$ and with second order MPT, $C_h(q)(T < T_c) > C_h(q)(T > T_c)$. In addition, $C_h(q)$ diverges at a finite wavevector $q_c \sim 2\pi/\zeta$. Nonetheless, $C_h(q)$ remains continuous across $T = T_c$ even with $\lambda < 0$. These results are summarised in the form of schematic figures in Fig. 4.

(iii) In case of first order MPT, $C_h(q)(T < T^*) < C_h(q)(T > T^*)$ with $\lambda > 0$, and $C_h(q)(T < T^*) > C_h(q)(T > T^*)$ with $\lambda < 0$. However, unlike across second order MPT, the difference $C_h(q)(T > T^*) - C_h(q)(T < T^*)$ does not vanish as $T \rightarrow T^*$. Thus, $C_h(q)$ is *discontinuous* across $T = T^*$, a consequence of the discontinuity of σ_a or κ_e . Qualitatively, the behaviors across the transition temperature T^* are similar to those for second order MPTs.

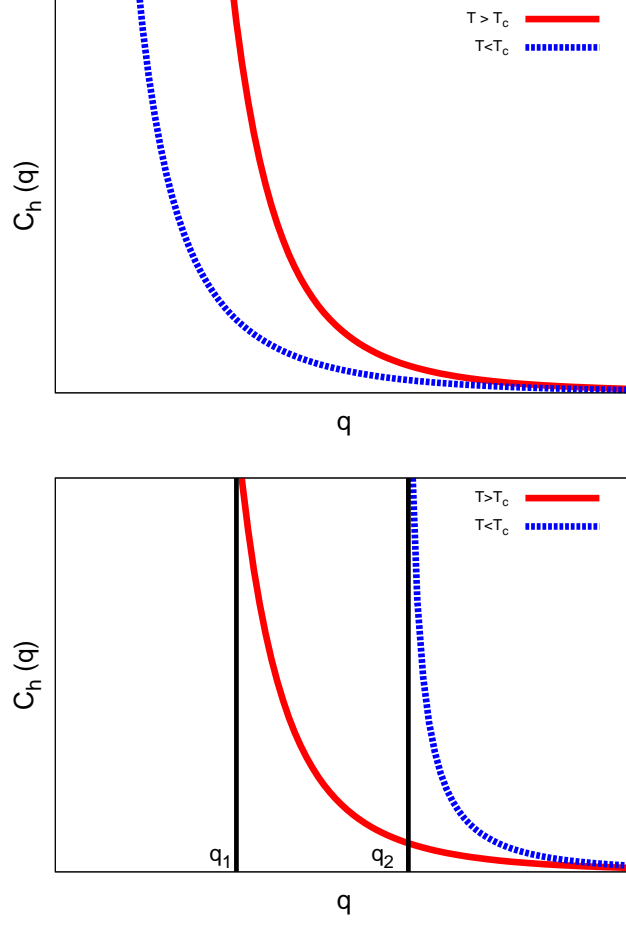


FIG. 4: Schematic scaling of $C_h(q)$ with q across second order MPTs: (top) $\lambda > 0$: red (solid) and blue (broken) curves represents $C_h(q)$ in the disordered ($T > T_c$) and ordered ($T < T_c$) phases, respectively; $C_h(q)$ diverges only when $q \rightarrow 0$ for both $T > T_c$ and $T < T_c$ (see text). (bottom) $\lambda < 0$: red (solid) and blue (broken) curves represents $C_h(q)$ in the disordered ($T > T_c$) and ordered ($T < T_c$) phases, respectively. Finite wavevector singularities of $C_h(q)$ at wavevectors $q_1 = 2\pi/\zeta_{T>T_c}$ and $q_2 = 2\pi/\zeta_{T<T_c}$ with ζ following Eq. (28) are visible.

The changes in the membrane conformations with λ , characterised by Δ_n , Δ_h at a fixed T may be viewed as a *nonequilibrium structural phase transition* between soft and stiff phases (see Fig. 5). An order parameter for this transition may be constructed as in [17, 37].

C. Effects of a finite surface tension

If the membrane has a finite surface tension $\sigma > 0$, then it generically suppresses h -fluctuations. Equation (8), in the presence of a finite surface tension σ , now modifies to

$$\frac{\partial h}{\partial t} = \Gamma_h [-\kappa \nabla^4 h + (\sigma + \lambda \phi^2 + \tilde{\lambda} \phi) \nabla^2 h] + f_h, \quad (29)$$

The equilibrium terms (29) can be obtained from the free energy \mathcal{F} , now supplemented by contributions from σ . Extracting an active tension σ_a from (29) using the logic outlined above, we find that the dynamics is controlled by the total tension σ_{tot} that includes both the active tension and σ ,

$$\sigma_{tot} = \sigma + \sigma_a > (<) \sigma \text{ for } \sigma_a > (<) 0, \quad (30)$$

where σ_a is defined as in Eq. 15. A positive σ_{tot} ($\lambda > 0$) necessarily suppresses membrane fluctuations. Thus, for $\sigma_a > 0$, the role of a non-zero σ is to suppress membrane fluctuations further. For $\sigma_a < 0$ ($\lambda < 0$), crumpling

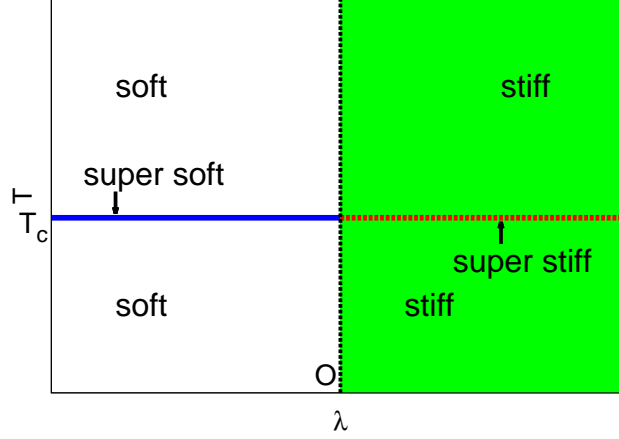


FIG. 5: (Color online) Schematic phase diagram in the $\lambda - T$ plane ($\tilde{\lambda} = 0$). Super-stiff and super-crumpling lines are marked. The solid horizontal (blue) and broken vertical lines refer to $T = T_c$ and $\lambda = 0$, respectively. Symbol O marks the origin $(0, 0)$.

instabilities should set in only for $\sigma_{tot} = 0$. Ignoring $\tilde{\lambda}$, this now yields a non-zero threshold of instability for $|\lambda| \propto \sigma$ for all T with first order MPT and $T \neq T_c$ with second order MPT:

$$\lambda = -\frac{\sigma}{\langle \phi^2 \rangle} \quad (31)$$

determines the instability threshold of σ . For $T \approx T_c$ with second order MPT, $\langle \phi^2 \rangle$, and hence σ_a diverges with L as $\ln L$; thus the threshold of instability of λ vanishes in TL. In the more general case, one may consider a composition-dependent surface tension $\sigma(\phi)$. Using a simple form for $\sigma(\phi)$, it has been argued in Appendix F that the active terms continue to dominate in the hydrodynamic limit and thus our results still hold. For a tensionless lipid membrane that undergoes only a second order MPT in equilibrium, $\sigma(\phi) = 0$ identically.

IV. NATURE OF MPTS

There is no general framework available to study phase transitions in nonequilibrium systems. Nonetheless we are able to analyse the MPTs here by drawing analogy between the effective theory for composition fluctuations and standard equilibrium results.

Regardless of the nature of MPTs, we have for a symmetric membrane $\langle \nabla^2 h \rangle = C = 0$. Now, ignoring height fluctuations, if we substitute $\nabla^2 h$ by $C = 0$ in (9), it reduces to the standard equilibrium, conserved dynamics (model B in the nomenclature of Ref. [8]), corresponding to the free energy (6) [with $h = \text{const.}$] that yields phase behaviour identical to the standard liquid gas transition at temperature D_ϕ : phase coexistence for $r < 0$ or $T < T_c$ with an asymmetric coexistence curve about the critical density and a critical point at $T = T_c$ belonging to the $2d$ Ising universality class [9]. Thus any active modification of this equilibrium-like picture should be fluctuation induced. To investigate that further, we follow Ref. [39] and perturbatively integrate out h -fluctuations and obtain an effective dynamical equation for ϕ only. Operationally, to account for the fluctuation effects at the simplest level, we calculate the effective (fluctuation-corrected) parameters of (9) at the lowest order in perturbative expansions. We then express (9) in terms of the fluctuation-corrected parameters and substitute $\nabla^2 h$ by $\langle \nabla^2 h \rangle (= 0)$, ignoring fluctuations. In this approximation, the ϕ -dynamics is entirely described by a fluctuation-corrected free energy F_ϕ , entirely decoupled from h which has the form

$$F_\phi = \int d^d x \left[\frac{r}{2} \phi^2 + \frac{g_e}{3} \phi^3 + \frac{u_e}{4} \phi^4 + \frac{v}{6} \phi^6 - \tilde{h} \phi \right], \quad (32)$$

with

$$\frac{\partial \phi}{\partial t} = \Gamma_\phi \nabla^2 \frac{\partial F_\phi}{\partial \phi} + \nabla \cdot \mathbf{f}_\phi \quad (33)$$

as the attendant effective dynamical equation for ϕ . In (32), u_e and g_e include one loop corrections to the bare couplings u and g , respectively. Here we have ignored the corrections to r and v since these are not central to the

analysis here; a correction to r merely shifts T_c and we assume v is always positive. Further, \tilde{h} has no active corrections at the lowest order. Thus the one-loop effective dynamics of ϕ follows the equilibrium model B dynamics with free energy F_ϕ at an effective temperature D_ϕ .

With $\lambda > 0$, retaining only the inhomogeneous *active* one-loop correction to u and g (this suffices for our arguments here) we obtain $u_e = u + \Delta u = u + \lambda_p \tilde{\lambda}^2 D_h A$ and $g_e = g + \tilde{\lambda}^2 \lambda_2 D_h B_1 + \lambda \lambda_2 D_h B_2$ where, $\lambda_p = \lambda_2 \tilde{\lambda}$ and A, B_1, B_2 are numerical constants; see Appendix C. Thus effective couplings u_e and g_e can be independently positive, negative or zero.

The phase behaviour and transitions of ϕ can be directly obtained from F_ϕ . First consider $u_e > 0$. The term $v\phi^6$ in (32) is now redundant and we ignore it. Then F_ϕ has the same form as \mathcal{F} in (6). As a result, the discussions that immediately follow \mathcal{F} apply to F_ϕ as well: by making a suitable shift in ϕ , the cubic term $g_e \phi^3$ may be eliminated from F_ϕ , yielding a modified form for F_ϕ identical to the free energy for the Ising model in the presence of an external magnetic field \tilde{h}_ϕ . Then, composition ϕ generally undergoes a first order MPT below a transition temperature. A critical point with a second order MPT may be accessed only by suitable tuning of *both* T and \tilde{h}_ϕ : in fact the critical point is located in the (T, \tilde{h}_ϕ) plane at $r = 0$ or $T = T_c$ and $\tilde{h}_\phi = 0$, with an associated universal scaling behaviour belonging to the $2d$ Ising universality class [9]. Since \tilde{h}_ϕ in general does depend on the active coefficients $\lambda, \tilde{\lambda}$, tuning activity can make $\tilde{h}_\phi = 0$. Further, T_c too receives fluctuation corrections that depends on activity (not shown here). Thus the critical point for this nonequilibrium second order MPT can be accessed by controlling the activity. The role of $g_e \neq 0$ is only to introduce an asymmetry of the order parameter $\langle \phi \rangle = m$ about the critical density, reflected in the curvature of the coexistence curve at the criticality [9]. Since g_e can be varied continuously and made positive, negative or zero by tuning the composition-membrane interactions parameters, the curvature at criticality and hence the location of the coexistence curve in the $\phi - D_\phi$ plane changes continuously with the active parameters. Experimental measurements of the coexistence curve for a given system can thus reveal valuable quantitative information about the active coefficients and the underlying active processes in the membrane.

To ensure thermodynamic stability for $u_e < 0$, we need to include the $v\phi^6$ -term into consideration. This then yields a first order MPT at temperature $T^* = T_c + 2u_e^2/(3v)$ and $m^2 = |u_e|/(2v)$ even for $\tilde{h}_\phi = 0$ in direct analogy with the known equilibrium MF results [9]. At the tricritical point, $u_e = 0$, i.e., $u = -\lambda_p \tilde{\lambda}^2 D_h n A$ and $\tilde{h}_\phi = 0$. Notice that, unlike equilibrium examples of tricritical points [9], here the condition for the tricritical point explicitly involves D_h , thus bearing the hallmark of nonequilibrium [40]. While the MPTs for $u_e > 0$ are essentially indistinguishable from their equilibrium counterparts or the equilibrium liquid-gas phase transitions with a second order MPT accessible by setting $\tilde{h}_\phi = 0$ and tuning T to T_c , the prospect of a first order MPT for $u_e < 0$ at $\tilde{h}_\phi = 0$ at $T = T^* > T_c$ and the associated tricritical point are truly remarkable in that they have no analogues in the equilibrium limit of the MPTs or in the equilibrium liquid-gas phase transition. Fluctuation induced shifts in T_c and T^* due to $\lambda_p \neq 0$ are argued to be finite (see Appendix), suggesting T_c and T^* to be experimentally accessible at least for certain inversion-symmetric mixed membranes with proper choices for the model parameters. A schematic phase diagram of the model in the $\lambda_p - u$ plane with $\lambda > 0$ and $\tilde{h}_\phi = 0$) is shown in Fig. 6. Our analysis of MPTs are only indicative in nature that may

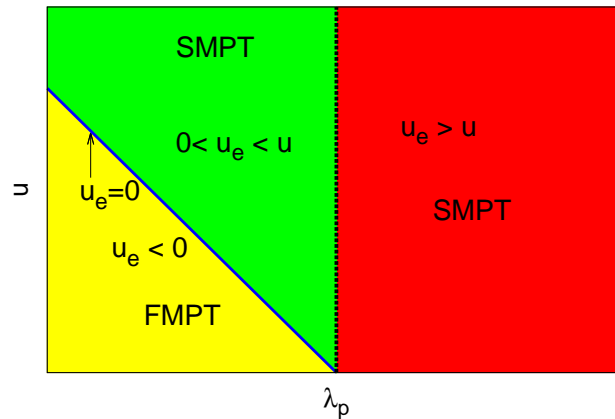


FIG. 6: (Color online) Schematic phase diagram in the $\lambda_p - u$ plane ($\lambda, u > 0, \tilde{h}_\phi = 0$). Inclined blue line marks the line of tricritical points (boundary between first order MPT and second order MPT : $u_e = 0$; see text). The vertical broken line (separating the red and green regions) represents $u_e = u$.

be confirmed by detailed numerical studies.

V. SUMMARY AND OUTLOOK

We have thus developed an active hydrodynamic theory for inversion-symmetric mixed membranes. There may be a variety of physical realisations which may be described by our model in the hydrodynamic limit, e.g., a mixed symmetric lipid membrane immersed in an isotropic active fluid or a mixed symmetric lipid membrane with an active component in a passive fluid. We demonstrate that the interplay between heterogeneity and the active processes in the form of lipid-dependent active tensions leads to nontrivial fluctuation properties of mixed membranes. We establish a direct correspondence between membrane conformation fluctuations and MPTs in mixed lipid membranes, which forms a key result of this work. This can be tested in *in-vitro* experiments on various physical realizations of our model; membrane fluctuations may be measured by spectroscopic methods [38]. In particular, tagged particle diffusion measurements [7] may be used to validate our results. We welcome construction of lattice-gas type nonequilibrium models which will be particularly suitable to numerically study and verify the results obtained here; see, e.g., Ref. [41]. Our work clearly provides a way to ascertain the sign of λ and the nature of MPTs *without* measuring ϕ -fluctuations. For a jump in σ_a or κ_e at a given $T = T^*$, it must be first order MPT; else if σ_a or $\kappa_e(q)$ rises smoothly and diverges at some $T = T_c$ as $q \rightarrow 0$, the system displays second order MPT. Furthermore, if $\sigma_a|_{disorder} < (>) \sigma_a|_{order}$, or equivalently, $\kappa_e|_{disorder} < (>) \kappa_e|_{order}$, then $\lambda > (<) 0$. A mixed lipid membrane immersed in an active isotropic fluid made of actin filaments is a possible *in vitro* system to study our theory. This may be possible by reconstituted actomyosin arrays on a liposome; see, e.g., Ref. [42] for a related experimental study. ATP depletion methods [43] can be used to control the magnitude of λ and $\tilde{\lambda}$. It would be interesting to see how contractile or extensile active fluids [10] affect the couplings $\lambda, \tilde{\lambda}$. The sign of λ_p , crucial in our theory for fixing the order of MPT, may be varied by using different sets of lipids. It may be noted that in the ordered phase separated state with A- and B-rich domains, one may define a κ_e in a given domain that is A- or B-rich. Measurement of this domain-dependent κ_e can further yield information about both $\lambda, \tilde{\lambda}$; see Appendix.

So far in the above, we ignored hydrodynamic friction [44]. Even when that is included in our analysis, our general conclusion of a one-to-one correspondence between the membrane conformation fluctuations and the nature of the MPTs holds good. Interestingly with hydrodynamic friction, our results hold true even if the membrane is *impermeable*, i.e., $v_{perm} = 0$; see Appendix. We have neglected the geometric nonlinearities in our analysis above. These originate from the nonlinear forms of the area element and mean curvature in the Monge gauge; see Ref. [18]. These are irrelevant near the critical point in a scaling sense in the presence of the existing nonlinearities. Across first order MPT these may affect the first order transition temperature T^* and order parameter m quantitatively; however, our general conclusions are expected to remain unchanged. We did not include any ϕ^3 or ϕ^5 term in (6) above, as we considered only second order MPT belonging to the Ising universality class in the equilibrium limit. A ϕ^3 -term in (6) above would yield a first order MPT in equilibrium; a ϕ^5 -term would be irrelevant in a scaling sense in the presence of the ϕ^4 -term in (6) above. Beyond its immediate applicability to suitable *in-vitro* systems, our theory should serve as a basis for studying the physics of phase transitions in live cell membranes. We expect our theory to introduce new directions in the physical understanding of living cell membrane dynamics with new vistas of striking nonequilibrium phenomena. We look forward to experimental tests of our predictions on GPMVs and live cell membrane extracts.

VI. GLOSSARY: Δ_n, Δ_h AND ζ FOR FIRST ORDER MPT AND SECOND ORDER MPT

Below we provide a list of symbols and the principal results that form the basis of this work here.

$$\Delta_h = \int_{2\pi/L}^{\Lambda} \frac{d^2 q d\Omega}{(2\pi)^3} \langle |h(q, \Omega)|^2 \rangle, \quad (34)$$

where Ω is a frequency and $\langle |h(q, \Omega)|^2 \rangle = \frac{\langle |f_h(q, \Omega)|^2 \rangle}{\Omega^2 + \Gamma_h^2 \kappa_e^2 q^8} = \frac{2D_h \Gamma_h}{\Omega^2 + \Gamma_h^2 \kappa_e^2 q^8}$. Similarly,

$$\Delta_n = \int_{2\pi/L}^{\Lambda} \frac{d^2 q d\Omega}{(2\pi)^3} q^2 \langle |h(q, \Omega)|^2 \rangle \quad (35)$$

We first assume $\lambda > 0$. The membrane becomes generically stiff for all T .

Case I : first order MPT at $T = T^*$, ($\lambda_p < 0$; see main text). At all T

(i) Δ_n : finite. \Rightarrow orientational LRO.

(ii) $\Delta_h \sim \ln L \Rightarrow$ positional QLRO.

(iii) Effective bending modulus, κ_e shows a jump across T^* : $\kappa_e(T > T^*) < \kappa_e(T < T^*)$.

Case II: second order MPT at $T = T_c$.

For any $T \neq T_c$,

(i) Δ_n is finite and smooth (no jump across T_c) \Rightarrow : orientational LRO.

(ii) $\Delta_h \sim \ln L \Rightarrow$: positional QLRO.

(iii) At $T = T_c$, Δ_n : finite (orientational LRO), in fact further suppressed than its value at $T \neq T_c$. On the other hand, $\Delta_h \sim \ln \ln L$ at $T = T_c$, \Rightarrow positional NLO.

(iv) Effective bending modulus, κ_e rises smoothly as T_c is approached.

Now assume $\lambda < 0$: Generic crumpling is introduced at all T giving a finite persistence length.

(i) second order MPT: $\zeta(T < T_c) < \zeta(T > T_c)$; $\zeta(T = T_c) \ll \zeta(T \neq T_c)$. $\zeta(T = T_c)$ follows the equation

$$\zeta^2 \ln(\zeta/2\pi) = \frac{8\pi^3 \kappa}{D_\phi |\lambda|}. \quad (36)$$

(ii) first order MPT: $\zeta(T < T^*) < \zeta(T > T^*)$.

VII. ACKNOWLEDGEMENT

The authors thank the Alexander von Humboldt Stiftung, Germany for partial financial support through the Research Group Linkage Programme (2016).

Appendix A: The active terms

We now briefly discuss a more formal derivation of the active terms. To this end, we closely follow Ref. [12], keeping the example in mind of a lipid membrane embedded in an isotropic active fluid made of actin filaments and motors. In the Monge gauge for a nearly planar membrane along the xy -plane, we can write for the local membrane velocity v_z as appropriate for a symmetric membrane (set $\sigma = 0$)

$$\frac{\partial h}{\partial t} = v_z = v_{hydroz} + X(\phi) \nabla_j (p_z p_j) - \Gamma_h \frac{\delta \mathcal{F}}{\delta h}. \quad (A1)$$

We use $p_i = \partial_i h$, $i = x, y$ at the location of the membrane; v_{hydroz} is the z -component of the three-dimensional hydrodynamic velocity \mathbf{v}_{hydro} . This may be formally justified by closely following the arguments outlined in Ref. [12]. We assume that the free energy is dissipated at a rate $\mathcal{R} \Delta \mu$, where \mathcal{R} is the reaction rate of ATP hydrolysis and $\Delta \mu$ is as given in the main text. Now treat v_z and \mathcal{R} as fluxes, and $\delta \mathcal{F}/\delta h$ and $\Delta \mu$ as the corresponding conjugate thermodynamic forces. Then as in Ref. [12], together with the condition for a symmetric membrane, we identify $\bar{\zeta} \nabla_j (p_z p_j) \delta \mathcal{F}/\delta h$ as the leading order contribution to \mathcal{R} up to the first order in gradients, where $\bar{\zeta}$ is an Onsager coefficient. Using the symmetry of the dissipative Onsager coefficients, we then set $\bar{\zeta} \nabla_j (p_z p_j) = X(\phi) \nabla_j (p_z p_j)$, giving a justification of the active terms.

Appendix B: Effective bending modulus

In general, from Eq. (8) (after neglecting fluctuations $\delta X(\phi)$ w.r.t. the mean value $\langle X(\phi) \rangle$), we obtain

$$\sigma_a = \lambda \langle \phi^2 \rangle + \tilde{\lambda} \langle \phi \rangle, \text{ or, } \kappa_e(q) = \kappa + \frac{\lambda}{q^2} \langle \phi^2 \rangle + \frac{\tilde{\lambda}}{q^2} \langle \phi \rangle. \quad (B1)$$

We have $\langle \phi \rangle = 0$, considering the whole system with equal amount of A and B lipids in the system. Now, the ordered phase is characterised by finite (macroscopic) size domains, which are A-rich or B-rich, for $T < T_c$ (second order MPT) or $T < T^*$ (first order MPT). This allows us to define σ_a or κ_e over a single (macroscopic size) domain, either A or B rich with average of ϕ in a given type of domain being non-zero; σ_a (or, κ_e) will now depend explicitly on the domain type. We now define domain-dependent active tensions σ_a^A and σ_a^B for A- and B-rich domains in the ordered phase and find

$$\sigma_a^A = \lambda \langle \phi^2 \rangle_A + \tilde{\lambda} \langle \phi \rangle_A, \quad \sigma_a^B = \lambda \langle \phi^2 \rangle_B + \tilde{\lambda} \langle \phi \rangle_B. \quad (B2)$$

Here, $\langle \dots \rangle_{A,B}$ represents averages taken in an A or B rich domain, respectively. For simplicity, let us consider just two macroscopic size domains, one A-rich and another B-rich. Within a simple mean-field like description, we define

an A (B) rich domain formally by $\langle\phi\rangle_A = m > 0$ ($\langle\phi\rangle_B = -m < 0$) and set $\tilde{\lambda} > 0$, $\lambda > 0$. Evidently, for sufficiently large $\tilde{\lambda}$, $\sigma_a^B < 0$. One may then define a threshold $\tilde{\lambda}_c$, given by $\sigma_a^B = 0$. This yields that a crumpling instability takes place in the B-rich domain for $\tilde{\lambda} > \tilde{\lambda}_c$ for a given size of the B-rich domain, where as σ_a remains positive in the A-rich domain and thus, the latter should be statistically flat. This is testable in experiments. In contrast, with $\lambda < 0$, the crumpling instability in the A-rich domain in the ordered phase may be suppressed by a sufficiently large $\tilde{\lambda}$, such that $\sigma_a^A > 0$ even with $\lambda < 0$. This corresponds to a novel situation, where a large enough flat mixed membrane as a whole is unstable in the disordered phase (since $\lambda < 0$), but a macroscopic part of it (i.e., the A-rich domain) gets stabilised and shows statistical flatness in the ordered phase (large $\tilde{\lambda} > 0$). Again, this should be testable in standard experiments. Overall we conclude that the stability and flatness of the mixed membrane, both in the disordered and ordered phases, depend very sensitively on the active processes. Since there are no domains in the disordered phase, the term with coefficient $\tilde{\lambda}$ has no effect on σ_a in the disordered phase, independent of first order MPT or second order MPT. Thus, the sign of σ_a is necessarily controlled by λ in the disordered phase and our results in main text directly apply. For sufficiently small $\tilde{\lambda}$, note that the results do not change qualitatively, and Eq. (15) remains valid in each domain.

Appendix C: Analysis of the MPTs : Active inhomogeneous fluctuation corrections to u and g

We begin with the generating functional [45] \mathcal{Z} corresponding to the Eqs. of motion (8) and (9). We find

$$\mathcal{Z} = \int \mathcal{D}h \mathcal{D}\hat{h} \mathcal{D}\phi \mathcal{D}\hat{\phi} \exp(S), \quad (\text{C1})$$

where the action functional

$$\begin{aligned} S = & \int d^d x dt \left[\frac{D_h}{\Gamma_h} \hat{h} \dot{h} - \hat{h} \left(\frac{1}{\Gamma_h} \frac{\partial h}{\partial t} + \kappa \nabla^4 h - \lambda \phi^2 \nabla^2 h - \tilde{\lambda} \phi \nabla^2 h \right) + \hat{\phi} \left(\frac{-D_\phi \nabla^2}{\Gamma_\phi} \right) \hat{\phi} - \hat{\phi} \left(\frac{1}{\Gamma_\phi} \frac{\partial \phi}{\partial t} \right. \right. \\ & \left. \left. - \nabla^2 [r\phi - \nabla^2 \phi + g\phi^2 + \frac{u}{3!} \phi^3 + 2\lambda_1 \phi (\nabla^2 h)^2 + \lambda_2 (\nabla^2 h)^2 + v\phi^5] \right) \right] \end{aligned} \quad (\text{C2})$$

One can then formally integrate out h and \hat{h} , and define an effective action functional S_ϕ as follows:

$$\exp(S_\phi) = \int \mathcal{D}h \mathcal{D}\hat{h} \exp(S). \quad (\text{C3})$$

To evaluate S_ϕ , we proceed perturbatively and then extract F_ϕ [39], such that the effective ϕ -dynamics is now given by Eq. (32). Ignoring the fluctuation corrections of Γ_ϕ and D_ϕ , as these are not central to the discussion here, we find

$$F_\phi = \int d^d x \left[\frac{r_e}{2} \phi^2 + \frac{1}{2} (\nabla \phi)^2 + \frac{g_e}{\phi} + \frac{u_e}{4} \phi^4 + \frac{v_e}{6} \phi^6 \right], \quad (\text{C4})$$

where a subscript e refers to fluctuation-corrected parameters. The corresponding effective equation of motion of ϕ is

$$\frac{\partial \phi}{\partial t} = \Gamma_\phi \nabla^2 \frac{\delta F_\phi}{\delta \phi} + \nabla \cdot \mathbf{f}_\phi. \quad (\text{C5})$$

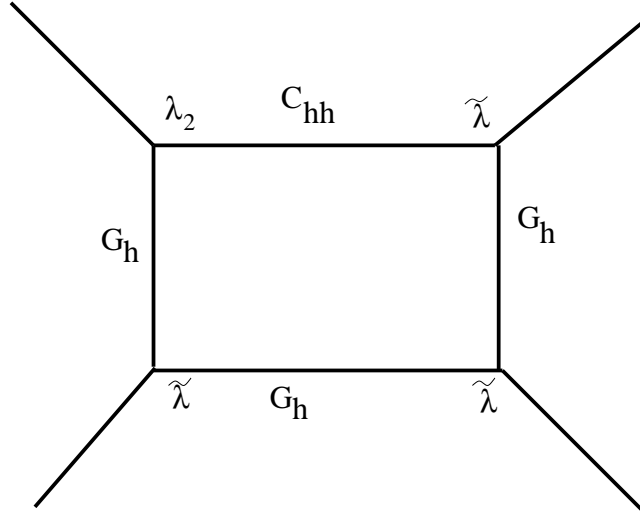
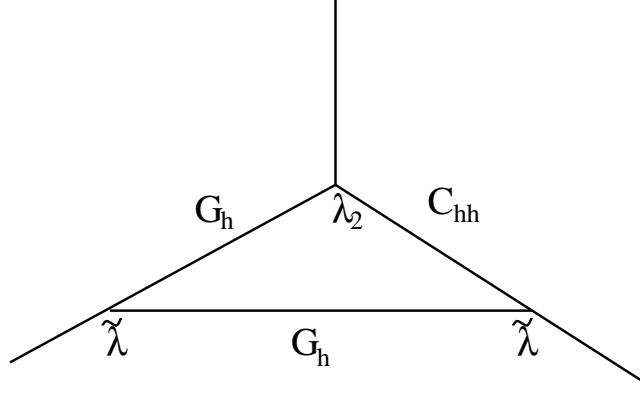
In our analysis in the main text, we ignore the difference between r_e and r , and between v_e and v , as these are of no significance to the mean-field like arguments used in the main text. We always assume $v > 0$. We also ignore the corrections to D_ϕ , since that just changes the effective temperature and is of no direct consequences here. Furthermore, there are no one-loop corrections to Γ_ϕ , owing to the conservation law form of (9).

To proceed further, we now need to find g_e and u_e perturbatively. The lowest order active inhomogeneous fluctuation corrections to g and u may be represented by the following Feynman diagrams; see Figs. 8, 9 and 7 below.

The correlator function for h , written in terms of the effective bending modulus $\kappa_e(q)$, is given by $C_{hh}(q, \Omega) = \langle |h(\mathbf{q}, \Omega)|^2 \rangle = \frac{2D_h \Gamma_h}{\Omega^2 + \Gamma_h^2 \kappa_e^2 q^8}$. In addition, $G_\phi(q, \Omega) = \frac{1}{-i\Omega + \Gamma_\phi q^2 (r + q^2)}$ and $G_h(q, \Omega) = \frac{1}{-i\Omega + \Gamma_h \kappa_e q^4}$ are the propagators for ϕ and h , respectively.

Furthermore, we assume $\lambda > 0$ for stability. The one-loop correction, Δu (see main text), thus evaluates to the following at $2d$:

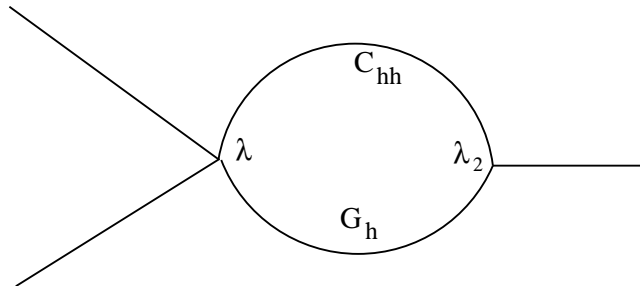
$$\Delta u = \frac{3\lambda_p \tilde{\lambda}^2 D_h}{4} \int_{2\pi/L}^\Lambda \frac{d^2 q}{(2\pi)^2 \kappa_e^4 q^6} \quad (\text{C6})$$

FIG. 7: Active fluctuation correction to u due to $\tilde{\lambda}, \lambda_2$.FIG. 8: Active fluctuation correction to g due to $\tilde{\lambda}, \lambda_2$.

Since $\kappa_e(q) \sim O(1/q^2)$ for sufficiently small q , Δu is clearly a finite contribution at TL, as argued for in the main text. Similarly, the one-loop correction, Δg of g , at $2d$ evaluates to

$$\Delta g = \frac{\tilde{\lambda}^2 \lambda_2 D_h}{2} B_1 + 2\lambda \lambda_2 D_h B_2, \quad (\text{C7})$$

where, $B_1 = \int_{2\pi/L}^{\Lambda} \frac{d^2 q}{(2\pi)^2} \frac{1}{2\kappa_e^2 q^4}$ and $\Delta_2 = \int_{2\pi/L}^{\Lambda} \frac{d^2 q}{(2\pi)^2} \frac{2}{\kappa_e^2 q^2}$ are finite in $2d$. The sign of Δu can thus be varied by varying

FIG. 9: Active fluctuation correction to g due to λ, λ_2 .

λ_p ; for sufficiently negative large λ_p , u_e can be made negative. Similarly, the sign of Δg may be varied and may be made positive, negative or zero by tuning λ_2 .

Appendix D: DRG flow equations and fixed points

Large critical point fluctuations very close to second order MPT may be systematically handled within dynamic renormalization group (DRG) frameworks; see Ref. [9] for technical details. With $\tilde{\lambda} = 0 = \lambda_2$, simple power counting shows that the nonlinear coefficients λ and u are *equally relevant* (in a scaling/DRG sense) at $2d$, the physically relevant dimension, with both being *marginal* at $d = 4$. This calls for a perturbative DRG calculation to be performed on Eqs. (8) and (9), together with an ϵ -expansion, $\epsilon = 4 - d$; see Ref. [9]. In this limit, the model admits only second order MPT belonging to the $2d$ Ising universality class. The one-loop DRG procedure formally involves the following steps (i) obtaining the one-loop fluctuation corrections to the different model parameters by integrating out the high wavevector parts of the fields from Λ/b to Λ , $b > 1$, (ii) rescaling the fields wavevector \mathbf{q} , frequency ω by $\mathbf{q}' = b\mathbf{q}$, $\omega' = b^z\omega$, where z is the dynamic exponent and rescaling of the fields h and ϕ accordingly [9]. The fixed points (FP) of the DRG are to be obtained from the flow equations for the relevant coupling constants in the problem, which in the present case are u and λ . The one-loop diagrams that contribute to u and λ are shown below in Fig. 10 and Fig. 11, respectively.

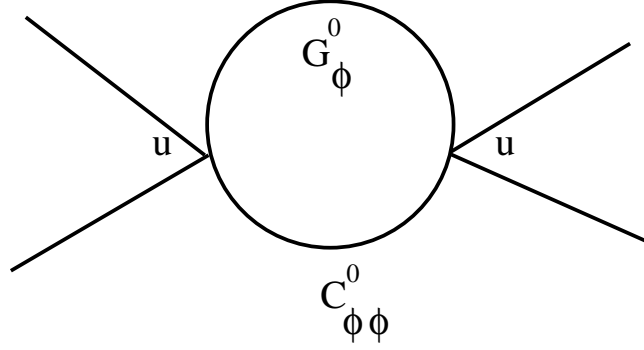


FIG. 10: Relevant one-loop correction to u . Here, $G_\phi^0 = \frac{1}{-i\Omega + \Gamma_\phi q^2(r+q^2)}$ and $C_{\phi\phi}^0 = \frac{2D_\phi\Gamma_\phi}{\Omega^2 + \Gamma_\phi^2 q^4(r+q^2)^2}$ are the bare propagator and correlator of ϕ , respectively.

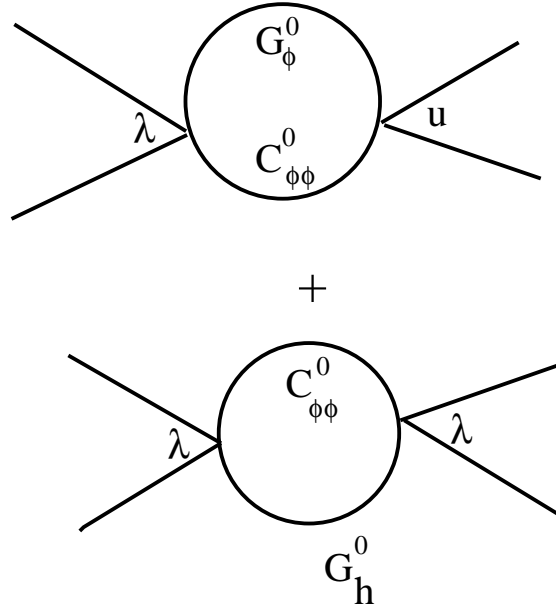


FIG. 11: Total correction to λ . Here, $G_h^0 = \frac{1}{-i\Omega + \Gamma_h \kappa q^2}$ is the bare propagator for h ; $C_{\phi\phi}^0$ and G_ϕ^0 are as in Fig. 10.

With $b = e^l \approx 1 + l$, $l \ll 1$, the resulting DRG recursion relations for u and λ yield

$$\frac{du}{dl} = u[\epsilon - 9uD_\phi], \quad (D1)$$

$$\frac{d\lambda}{dl} = \lambda[\epsilon - 3uD_\phi - 4\tilde{\Gamma}\lambda D_\phi], \quad (D2)$$

where $\tilde{\Gamma} = \frac{\Gamma_h}{\Gamma_\phi + \kappa\Gamma_h}$. For the flow equations (D1) and (D2), stable FP $u^* = \frac{\epsilon}{9D_\phi}$ and $\lambda^* = \frac{\epsilon}{6\tilde{\Gamma}D_\phi}$. Not surprisingly, $u^* = \epsilon/(9D_\phi)$ yields the critical exponents for the composition fluctuations at second order MPT identical to their values at the Heisenberg FP of the Ising model in equilibrium, consistent with the expectation that the second order MPT belongs to the Ising universality class. At the one-loop order, there are no fluctuation corrections to $\Gamma_h, \Gamma_\phi, D_h$ and D_ϕ . Now, since we are formally considering a tensionless membrane, noting that the leading order correction to the self-energy of $h(\mathbf{q}, \omega)$ is at $O(q^2)$, it is convenient to define $\tilde{\kappa}(q) = \kappa q^2$ ($\tilde{\kappa}$ clearly has the physical dimension of a surface tension), and obtain its fluctuation-corrections. We find

$$\frac{d\tilde{\kappa}}{dl} = \frac{\lambda D_\phi}{2\pi} \quad (D3)$$

as the DRG flow equation for $\tilde{\kappa}$. Solving this at the DRG FP, we obtain a scale-dependent, renormalised $\tilde{\kappa}(q)$ and thence, defining renormalised $\kappa_e(q)$ via $\tilde{\kappa}(q) = \kappa_e(q)q^2$,

$$\kappa_e(q) = \kappa + \frac{\lambda^* D_\phi}{q^2} \int_q^\Lambda \frac{d^2 q_1}{(2\pi)^2 q_1^2} \approx -\frac{\lambda^* D_\phi}{2\pi q^2} \ln q, \quad (D4)$$

at $d = 2$ for small q at the DRG FP or the critical point ($r = 0$). The one-loop correction to κ is shown in Fig. 12.

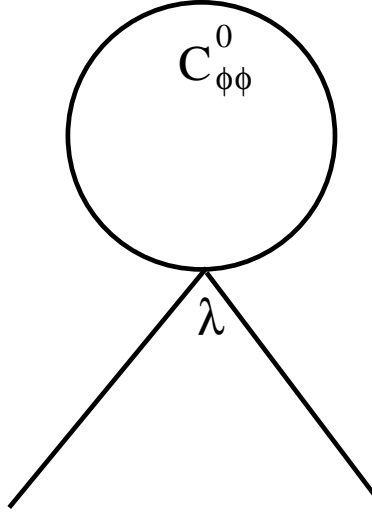


FIG. 12: One-loop correction to κ that yields $\kappa_e(q)$.

Here, at the DRG fixed point $\lambda^* D_\phi = \epsilon/(6\tilde{\Gamma})$. Then, $\Delta_n = -\frac{D_h}{\lambda^* D_\phi} \int_{q_0}^\Lambda \frac{q_1 dq_1}{\ln q_1}$, where $q_0 \sim 2\pi/L$ is the lower limit of the integral. The nature of the orientational order is determined by the L -dependence of Δ_n in the limit of large L (formally infinite at TL). Whether or not the limit $q_0 \rightarrow 0$ may be taken, depends on the behavior of the integrand, q_1 for $q_1 \rightarrow 0$. It can be shown in a straight forward way that for $q_1 \rightarrow 0$, $q_1/\ln q_1$ vanishes. Thus, we conclude that for $q_0 \sim 2\pi/L \rightarrow 0$, Δ_n remains finite. A precise numerical value of Δ_n may be obtained by numerical integrations. This, of course, will depend upon Λ , the upper limit. Since this is not particularly illuminating for the purposes of this work, we do not do this here. Furthermore, $\Delta_h = -\frac{2\pi D_h}{\lambda^* D_\phi} \int_{2\pi/L}^\Lambda \frac{d^2 q_1}{(2\pi)^2 q_1^2 \ln q_1} \approx \frac{D_h}{\lambda^* D_\phi} \ln \ln L$ in TL. Clearly, the amplitude $D_h/(\lambda^* D_\phi)$ is nonuniversal at the DRG FP and these results are in agreement with results obtained in the main text. Lastly, the lack of renormalization of Γ_h and Γ_ϕ at the one-loop order implies that dynamic exponent $z = 4$ at second order MPT for both h and ϕ , respectively (strong dynamic scaling).

Note that similar to u, λ and κ , r also receives fluctuation corrections, reflecting fluctuation-induced shift in T_c . Solving the DRG flow equation for r yields the correlation length exponent; see, e.g., Ref. [34]. Since this is not central to main issue of this work, we do not discuss this here.

In the above, we have worked up to the one-loop approximation. Notice however that the critical behaviour of ϕ follows the Ising universality class as elucidated above, and hence the equal-time correlator of ϕ is known *exactly* near the critical point from the exact solution of the $2d$ Ising model. We use this below to obtain the temperature-gradient of the renormalised bending modulus $\kappa_e(q)$ near the critical point $T = T_c$ (see also Refs [39, 46]). From Eq. (24), only the equal-time correlator $\langle \phi^2 \rangle$ enters into κ_e , giving [46]

$$\frac{\partial \kappa_e}{\partial T} = \lambda \frac{\partial}{\partial T} \langle \phi^2 \rangle \sim -C_v \quad (\text{D5})$$

near the critical point. For the $2d$ Ising model, $C_v \sim \ln(|T - T_c|/T_c)$ near T_c , yielding a logarithmic divergence [47]. This shows how $\kappa_e(q)$ diverges as $T \rightarrow T_c$. This in turn yields, upon integrating over temperature, $\kappa_e(q)$ has a diverging piece $\propto \ln(|T - T_c|/T_c)$ near the critical point. Now noting that that correlation length $\zeta_c \propto (|T - T_c|/T_c)^{-\nu}$ near T_c and setting $\zeta_c \sim 2\pi/q$ for the long wavelength modes, we find $\kappa_e(q) \propto \lambda q^2 \ln q$ in the long wavelength limit, in agreement with our one-loop result above.

In the above, although we have neglected λ_2 and $\tilde{\lambda}$, the effective coupling $\lambda_p = \tilde{\lambda}\lambda_2$ becomes marginal at $D = 4$, and hence should be *equally relevant* as u and λ in a DRG sense. Indeed, there are additional one-loop corrections to the various bare model parameters that originate from λ_p (not shown here). Nonetheless, as our one-loop effective free energy F_ϕ suggests, the critical behaviour of ϕ -fluctuations should still belong to the $2d$ Ising universality class. Thus, proceeding as above the divergence of $\kappa_e(q)$ near T_c remains unchanged.

Appendix E: Fluctuation induced shift in T_c

We now heuristically argue in favour of experimental accessibility of second order MPT and first order MPT in the system. Apart from the well-known shift in T_c due to the u -term in Eq.(9) [9], there is a correction to T_c of the form $\lambda_1 \langle (\nabla^2 h)^2 \rangle$, which is obviously finite. Additionally, a nonzero λ_p should lead to a fluctuation-induced shift in T_c . The corresponding one-loop Feynman diagram is shown in Fig. 13 below. The expression is of the form

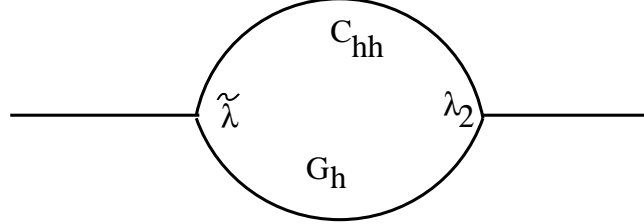


FIG. 13: Correction to T_c coming from λ_p . Clearly, this contribution being finite only produces a small shift.

$\sim \lambda_p D_h \int_{2\pi/L}^{\Lambda} \frac{d^2 q}{(2\pi)^2 \kappa_e^2 q^2}$, which is finite. Thus, the shift in the mean-field T_c due to the active effects is finite. This leads us to speculate that renormalised T_{cR} , i.e., the shifted or fluctuation-corrected T_c , should fall in a temperature range similar to the equilibrium critical points of model lipid bilayers, and correspondingly, any putative second order MPT should be accessible in experiments, at least for certain choices of the parameters of the model system. Furthermore, if we construct an effective Landau MF in terms of u_e and T_{cR} , the first order transition temperature T^* also gets a shift. Since T_{cR} is expected to be experimentally accessible, the shifted T^* should also be accessible experimentally for certain choices of the parameters of the model system. Thus, we speculate that it should be possible to observe MPTs (first order MPT or second order MPT) in certain inversion-symmetric lipid membranes, with properly tuned values of the model parameters, within experimentally accessible temperature ranges.

Appendix F: Composition-dependent surface tension

We now briefly consider the effects of a composition-dependent surface tension $\sigma(\phi)$. For simplicity we choose $\sigma(\phi) = \lambda_3 \phi^2 + \lambda_4 \phi$ in the free energy \mathcal{F} as given in (6). For reasons of thermodynamic stability, we choose $\lambda_3 > 0$; the sign of λ_4 is arbitrary and may be absorbed in the definition of ϕ . We choose the magnitude of λ_4 in a way to

ensure $\sigma(\phi) > 0$ for all ϕ , again to ensure thermodynamic stability. This now yields

$$\begin{aligned}\frac{\partial h}{\partial t} &= \Gamma_h[(\lambda\phi^2 + \tilde{\lambda}\phi)\nabla^2 h - \kappa\nabla^4 h + \lambda_3\nabla \cdot (\phi^2\nabla h) \\ &\quad + \lambda_4\nabla \cdot (\phi\nabla h)], \\ \frac{\partial \phi}{\partial t} &= \Gamma_\phi\nabla^2[r\phi - \nabla^2\phi + \frac{u}{3!}\phi^3 + 2\lambda_1\phi(\nabla^2 h)^2 + g\phi^2 \\ &\quad + \lambda_2(\nabla^2 h)^2 + v\phi^5 + (2\lambda_3\phi + \lambda_4)\nabla^2 h] \\ &\quad + \nabla \cdot \mathbf{f}_\phi.\end{aligned}\tag{F1}$$

Thus, compared to Eq. (8), there are additional terms with coefficients λ_3, λ_4 in Eq. (F1). Notice also that the term $\lambda_3\nabla \cdot (\phi^2\nabla h)$ has the same number of ϕ and h fields as in the active λ -term in Eqs. (8) or (F1); similarly, the term $\lambda_4\nabla \cdot (\phi\nabla h)$ has the same number of ϕ and h fields as in the active $\tilde{\lambda}$ -term in Eqs. (8) or (F1). Still, these λ_3 - and λ_4 -terms are total derivatives, whereas the active λ and $\tilde{\lambda}$ -terms are not. Thus in the hydrodynamic limit, the λ_3 - and λ_4 -terms may be neglected (in a scaling sense) in comparison with the λ and $\tilde{\lambda}$ -terms in (F1). It is important to note that if $\sigma(\phi)$ -term is included in \mathcal{F} , then the upper critical dimensions [9] of the λ_3 - and λ_4 -terms are 4 and 6, respectively. Thus, the MPT of the ϕ -fluctuations should no longer belong to the $2d$ Ising universality in the equilibrium limit. Given that in our work, we have considered a tensionless membrane that undergoes only second order MPT with $2d$ Ising universality at equilibrium, we set $\sigma(\phi) = 0$ identically in our work.

Appendix G: Hydrodynamic friction and active stresses

We now consider the effects of hydrodynamic friction, hitherto ignored, on the dynamics of a tensionless mixed membrane. We include the effects of an active (nonequilibrium) stress $\sigma_{ij} = \gamma(\phi)p_i p_j$ (see, e.g., Ref. [10]), that is generically present in an active fluid. (This ϕ -dependent active stress again reflects specific lipid dependence of the actin-lipid interactions.) With $p_z = 1, p_j = \partial_j h, j = x, y$, this makes a contribution of the form $\partial_j(\gamma(\phi)p_z p_j)$ to v_{hydroz} at $z = h$; see Ref. [12]. We now choose $\gamma(\phi) = A\phi^2 + B\phi$. Because of their active origins, there are no restrictions on the magnitudes and signs of A and B . If hydrodynamic damping is considered, Eq. (8) in the presence of the active stresses, modifies to [with the choice $X(\phi) = \Gamma_h(\lambda\phi^2 + \tilde{\lambda}\phi)$, see above.]

$$\begin{aligned}\frac{\partial h}{\partial t} &= -\mu_p \frac{\delta \mathcal{F}}{\delta h} + \Gamma_h[\lambda\phi^2\nabla^2 h + \tilde{\lambda}\phi\nabla^2 h] \\ &\quad + \Gamma'_h[-\frac{\delta \mathcal{F}}{\delta h} + A\nabla \cdot (\phi^2\nabla h) \\ &\quad + B\nabla \cdot (\phi\nabla h)] + f_h,\end{aligned}\tag{G1}$$

where Γ'_h is a damping coefficient. The terms within square brackets in (G1) with coefficients Γ'_h come from the solution of the three-dimensional hydrodynamic velocity field \mathbf{v}_{hydro} [12]:

$$v_{hydroz} = \Gamma'_h[-\frac{\delta \mathcal{F}}{\delta h} + A\nabla \cdot (\phi^2\nabla h) + B\nabla \cdot (\phi\nabla h)].\tag{G2}$$

For a constant Γ'_h , active terms with coefficients A and B in (G2) are total derivatives, and hence are subdominant (in a scaling sense) to those with coefficients $\lambda, \tilde{\lambda}$ in the hydrodynamic limit. Then, neglecting these A - and B - terms, we obtain Eq. (8) above. For hydrodynamic friction, $\Gamma'_h = 1/(4\eta q)$ in the Fourier space, where η is the ambient fluid viscosity (see Refs. [22, 44]). As a result the A - and B -terms no longer vanish in the hydrodynamic limit $q \rightarrow 0$, and hence compete with the active terms with coefficients $\lambda, \tilde{\lambda}$. Then, with $\Gamma'_h = 1/(4\eta q)$, the A - and B -terms contain *fewer* derivatives than the $\lambda, \tilde{\lambda}$ -terms and in a scaling sense should dominate over the λ - and $\tilde{\lambda}$ -terms, respectively. This may be shown in a formal way. Replace ϕ^2 by $\langle\phi^2\rangle$ and ϕ by $\langle\phi\rangle = 0$ in the rhs of (G1) above in a mean-field like approximation. This allows us to extract *two* active tensions:

$$\sigma_a^h = A\langle\phi^2\rangle, \quad \sigma_a = \lambda\langle\phi^2\rangle.\tag{G3}$$

The former is the *active hydrodynamic tension*, whereas the latter one is the active nonhydrodynamic tension [see Eq. (15)]. Equivalently, comparing with a tensionless isolated fluid membrane, we define an effective hydrodynamic bending modulus $\kappa_e^h = \kappa + A\langle\phi^2\rangle/q^2$, in analogy with Eq. (17). In the long wavelength limit, in terms of ignoring the nonlinear terms, the effective dynamics of h in the Fourier space is given by

$$\frac{\partial h(\mathbf{q}, t)}{\partial t} = -[\mu_p \kappa_e(q)q^4 + \frac{\kappa_e^h}{4\eta}q^3]h(\mathbf{q}, t) + f'_h.\tag{G4}$$

The zero-mean, Gaussian white noise f'_h should have a variance given by

$$\langle |f'_h(\mathbf{q}, \omega)|^2 \rangle = 2D_h + 2D'_h/q, \quad (\text{G5})$$

$D'_h > 0$. Equation (G4) then yields for the equal-time membrane height correlator

$$\langle |h(\mathbf{q}, t)|^2 \rangle = \frac{D_h + D'_h/q}{\mu_p \kappa_e q^4 + \kappa_e^h q^3 / (4\eta)}. \quad (\text{G6})$$

The active coefficients λ and A are formally independent of each other and can be positive or negative separately. As a result, a variety of situation may emerge. (i) If λ and A have the same sign - both positive or negative, we may neglect the λ -term in comparison with the A -term, and $\Gamma_h \kappa q^4$ in comparison with $\kappa q^3 / (4\eta)$ in (G6). Thus the long wavelength fluctuations of $h(\mathbf{q}, t)$ is now controlled by κ_e^h . Since A can be positive or negative (just like λ), κ_e^h varies with A yielding an L -dependence similar to that for κ_e in the main text. This evidently yields similar scaling behaviours for Δ_n and Δ_h (as defined in the main text) across first order MPT and second order MPT, with now A playing the role of λ in the main text. Thus, the correspondence between MPTs and the membrane conformation fluctuations that is elucidated above with just nonhydrodynamic friction, survives with hydrodynamic friction as well. Furthermore, for an impermeable membrane (for which $v_{perm} = 0$, i.e., $\lambda = 0 = \tilde{\lambda}$) with hydrodynamic friction, Δ_n and Δ_h behave the same way as above across second order MPT and first order MPT, again establishing the direct correspondence between membrane conformation fluctuations and MPT, now for an impermeable membrane. (ii) Different signs of A and λ : in this case, one would encounter instabilities. For instance, with $A < 0$ and $\lambda > 0$, the model displays instabilities at the smallest wavevectors, where for the opposite case ($A > 0, \lambda < 0$), the system remains stable at the smallest wavevectors, but shows finite wavevector instabilities controlled by the relative magnitudes of A and λ . To what degree A and λ can be independently controlled and the biological significance of these results can be studied numerically by using properly constructed atomistic models.

-
- [1] B. Alberts, D. Bray, J. Lewis, M. Raff, K. Roberts, J.D. Watson, *Molecular Biology of the Cell*, 3rd edition (Garland, New York, 1994).
 - [2] D. Mizuno *et al*, *Science* **315**, 370 (2007); B. Stuhmann *et al*, *Phys. Rev. E* **86**, 020901(R) (2012).
 - [3] M.-J. Huang, H.-Yi Chen, and A. S. Mikhailov, *Eur. Phys. J. E* **35**, 119 (2012); M.-J. Huang, R. Kapral, A. S. Mikhailov, and H.-Yi Chen, *J. Chem. Phys.* **138**, 195101 (2013); see also H. Lodish, A. Berk, C. A. Kaiser, M. Krieger, M. P. Scott, A. Bretscher, H. Ploegh, and P. Matsudaira, *Molecular Cell Biology*, 6th ed. (W. H. Freeman, 2007).
 - [4] S. Ramaswamy, J. Toner and J. Prost, *Phys. Rev. Lett.* **84**, 3494 (2000) discuss a study on protein pumps in a fluid membrane; the membrane in this work, however, is asymmetric under inversion, and hence different from ours.
 - [5] For recent reviews, see, e.g., F. A. Heberle and G. W. Feigen-son, *Cold Spring Harb Perspect Biol* **3**, 004630 (2011); K. Simons and J. L. Sampaio, *ibid.*, p. 4697; E. L. Elson *et al*, *Annu. Rev. Biophys.* **39**, 207 (2010); see also M.E.Cates and J. Tailleur, *Annu. Rev. Cond. Mat. Phys.*, **6**, 219 (2015), R. Wittkowski *et al*, *Nat. Comm.*, **5**, 4351 (2014) and J. Stenhammar *et al*, *Phys. Rev. Lett.*, **111**, 145702 (2013) for some recent studies on active MPTs.
 - [6] S. L. Veatch *et al*, *Proc. Natl. Acad. Sci. U.S.A.* **104**, 17650 (2007); S. L. Veatch, *ACS Chem. Biol.* **3**, 287 (2008); A. R. Honerkamp-Smith *et al*, *Biophys. J* **95**, 238 (2008); A. R. Honerkamp-Smith *et al*, *Biochimica et Biophysica Acta* **1788**, 53 (2009). R. Honerkamp-Smith, B. B. Machta and S. L. Keller, *Phys. Rev. Lett.* **108**, 265702 (2012).
 - [7] See, e.g., I. Lee *et al*, *J. Phys. Chem.* **119**, 4450 (2015) and references therein.
 - [8] P. C. Hohenberg and B. I. Halperin, *Rev. Mod. Phys.* **49**, 435 (1977).
 - [9] P. M. Chaikin and T. C. Lubensky, *Principles of condensed matter physics* (Cambridge University Press, Cambridge 2000).
 - [10] S. Ramaswamy, *Annu. Rev. Condens. Matter Phys.* **1**, 323 (2010); J.-F. Joanny, J. Prost, in *Biological Physics, Poincare Seminar 2009*, edited by B. Duplantier, V. Rivasseau (Springer, 2009) pp. 1-32; M. C. Marchetti, J. F. Joanny, S. Ramaswamy, T. B. Liverpool, J. Prost, M. Rao, and R. A. Simha *Rev. Mod. Phys.* **85**, 1143 (2013).
 - [11] T. C. Adhyapak, S. Ramaswamy, J. Toner, *Phys. Rev. Lett.* **110**, 118102 (2013); L. Chen and J. Toner, *Phys. Rev. Lett.* **111**, 088701 (2013).
 - [12] A. Maitra, P. Srivastava, M. Rao and S. Ramaswamy, *Phys. Rev. Lett.* **112**, 258101 (2014).
 - [13] S. Zhou *et al*, *Proc. Nat. Acad. Sci.* **111**, (2014).
 - [14] In-vitro model lipid bilayers are typically inversion-symmetric; see Ref. [6].
 - [15] We ignore the bilayer structure; see, e.g., E. J. Wallace *et al*, *Biophys J* **88**, 4072 (2005); T. Baumgart *et al*, *Annu. Rev. Phys. Chem.* **62**, 483 (2011).
 - [16] L. Peliti and S. Leibler, *Phys. Rev. Lett.*, **54**, 1690 (1985).
 - [17] T. Banerjee and A. Basu, *Phys. Rev. E* **91** 012119 (2015).
 - [18] *Statistical Mechanics of Membranes and Surfaces*, edited by D. Nelson, T. Piran, and S. Weinberg World Scientific, Singapore (1989).
 - [19] A. Safran, *Statistical Thermodynamics of Surfaces, Interfaces, and Membranes* (Westview Press, 2003).

- [20] G. S. Ayton, J. L. McWhirter, P. McMurtry and G. A. Voth, *Biophys J.*, **88**, 3855 (2005).
- [21] Actin filaments are known for lipid-specific interactions, e.g., phosphatidylinositol bisphosphate lipids promote actin polymerization on the membrane; see, e.g., Ref. [1]; see also J. Dinic *et al.*, *Biochimica et Biophysica Acta - Biomembranes* **1828**, 1102 (2013) for studies on lipid raft - actin filaments interactions.
- [22] W. Cai and T. C. Lubensky, *Phys. Rev. E* **52**, 4251 (1995).
- [23] In principle, there can be “active tension” terms in v_{hydroz} which can originate from *active stresses*; see, e.g., Ref. [12] above. For a membrane with a fixed background, i.e., with a constant Γ_0 these are just as relevant as the $\lambda, \tilde{\lambda}$ -terms considered in Eq. (8) and are ignored here. See Appendix for additional technical discussions for hydrodynamic damping; see also Ref. [44] below.
- [24] For the full nonequilibrium model, r is a temperature-like tunable parameter in the model; r may be tuned by controlling the ambient temperature. Obviously, r assumes the usual significance of thermodynamic temperature in the equilibrium limit.
- [25] To recover the correct equilibrium limit, one needs to drop the λ - and $\tilde{\lambda}$ -terms in (8) and reinsert the λ_1 - and λ_2 - terms in (8). The absence of the λ_1 - and λ_2 - terms in (8) does not affect our analysis of the active membrane fluctuations in the long wavelength limit.
- [26] We do not include *active* ϕ^2 -, or ϕ^3 -terms. Such terms would survive even for $h = const.$, where as active processes here are assumed to couple with the membrane via mean curvature $\nabla^2 h$, and hence all active effects on the membrane should vanish for $h = const.$. This rules out an active ϕ^2 term in Eq. (9). In any case, these are no more relevant (in a scaling sense) than those (of equilibrium origin) already exist in (9).
- [27] P.-G. de Gennes, J. Prost, *The Physics of Liquid Crystals* (Clarendon, Oxford, 1993).
- [28] N. Sarkar and A. Basu, *Eur. Phys. J E* **36**, 86 (2013).
- [29] By this we mean a nonvanishing relaxation rate of \mathbf{p} in the limit of wavevector $q \rightarrow 0$.
- [30] In general, $X(\phi)$ should have a ϕ -independent constant piece α that yields an effective surface tension term in (8); see below. We ignore this for simplicity.
- [31] C. Sykes, J. Prost, and J. F. Joanny, in *Actin-based Motility: Cellular, Molecular and Physical Aspects*, edited by Marie France Carlier (Springer, New York, 2010).
- [32] N. Gov, *Phys. Rev. Lett.* **93**, 268104 (2004).
- [33] P. Girard *et al.*, *Biophys. J.* **87**, 419 (2004).
- [34] N. Sarkar and A. Basu, *Phys. Rev. E* **92**, 052306 (2015).
- [35] N. Selve and A. Wegner, *J. Mol. Biol.* **187**, 627 (1986).
- [36] S. Katira *et al.*, *eLife* **5**, e13150 (2016).
- [37] T. Banerjee, N. Sarkar and A. Basu, *Phys. Rev. E* **92**, 062133 (2015).
- [38] T. Betz and C. Sykes, *Soft Matter* **8**, 5317 (2012).
- [39] A. T. Dorsey, P. M. Goldbart and J. Toner, *Phys. Rev. Lett.* **96**, 055301 (2006).
- [40] See, e.g., S. Lübeck, *J. Stat. Phys.* **123**, 193 (2006).
- [41] B. B. Machta *et al.*, *Biophys. J* **100**, 1668 (2011).
- [42] M. Murrell, T. Thoresen and M. Gardel, *Methods in Enzymology* **540**, 265 (2014).
- [43] P. Singh *et al.*, *Assay. Drug. Dev. Technol.* **2**, 161 (2004).
- [44] L. Kramer, *J. Chem. Phys.* **55**, 2097 (1971).
- [45] C. DeDominicis, *J. Phys. (Paris)* **37**, Colloque C-247 (1976).
- [46] J. A. Aronovitz, P. Goldbart and G. Muzurkewich, *Phys. Rev. Lett.* **64**, 2799 (1990).
- [47] L. Onsager, *Phys. Rev.* **65**, 117 (1944).